Concentration Probe Measurements in a Mach 4 Nonreacting Hydrogen Jet

D R Buttsworth

Faculty of Engineering and Surveying
University of Southern Queensland
Toowoomba, Qld, 4350
Australia
Email: buttswod@usq.edu.au
Fax: 61 7 4631 2526

T V Jones

Department of Engineering Science
University of Oxford
Oxford, OX1 3PJ
UK

Abstract

A new probe technique is introduced for the measurement of concentration in binary gas flows. The new technique is demonstrated through application of the probe in a Mach 4 nonreacting jet of hydrogen injected into a nominally quiescent air environment. Previous concentration probe devices have mostly used hot wires or hot films within an aspirating probe tip. However, the new technique relies on Pitot pressure and stagnation point transient thin film heat flux probe measurements. The transient thin film heat flux probes are operated at a number of different temperatures and thereby provide stagnation temperature and heat transfer coefficient measurements with an uncertainty of around ±5K and ±4% respectively. When the heat transfer coefficient measurements are combined with the Pitot pressure measurements, it is demonstrated that the concentration of hydrogen within the mixing jet can be deduced. The estimated uncertainty of the reported concentration measurements is approximately ±5% on a mass fraction basis.

Introduction

Concentration measurements are needed in many environments where mixing and combustion occurs. Non-intrusive laser-based techniques such as laser induced fluorescence are currently used in many laboratories to measure concentrations of species such as OH and NO. However, probe measurements can still make valuable contributions in many situations due to their low cost, and ease of installation and operation.

For concentration measurements in subsonic isothermal flows, various techniques based on hot wire anemometry have been demonstrated. For example, McQuaid and Wright [1,2] used exposed hot wire sensors for velocity and concentration measurements in subsonic jet flows. In general, at least two different overheat ratios are necessary if concentration measurements are to be obtained from exposed hot wire devices. However, if an aspirating probe is operated at choked conditions, then a single hot wire located within the probe is sufficient for concentration measurements provided the stagnation pressure and temperature do not vary. Brown and Rebollo [3]

developed such a probe for subsonic mixing layer measurements. Shock tube calibration tests indicated a response time of around 0.2ms for the Brown-Rebollo device [3].

For concentration measurements in compressible flows, aspirating devices have also been used. Swithenbank [4] discussed a concentration probe which utilised pressure transducers to monitor the flow rate through a choked orifice which was located downstream of the aspirating probe tip. Ninnemann and Ng [5] used a hot wire upstream of a choked orifice with independent measurements of total pressure and temperature to measure concentration variations across a compressible shear layer. The maximum bandwidth for aspirating probes is limited to around 20kHz because of the need to establish a quasi-steady choked flow within the probe [6,7].

The current article introduces a new probe technique for concentration measurements in binary gas flows. The probe arrangement utilises transient thin film heat flux gauge technology and represents a natural extension of the fast-response stagnation temperature probe technique that has been reported previously [8]. When operated as either a stagnation temperature probe or a concentration probe, the device is robust and is well suited to compressible flow measurements. In the current work, the operating principles are first discussed and then the technique is demonstrated by describing stagnation temperature and concentration measurements in a nonreacting hydrogen free jet arrangement.

Measurement Technique

Transient Thin Film Probes

Platinum films were hand-painted onto the rounded end of fused quartz rods with a diameter of about 3mm, as illustrated in Fig. 1. Three transient thin films were used in the present work. Low resistance gold leads were also painted onto the quartz and the active film length was less than 1mm in each case.

The films were operated in a constant current mode so that the voltage drop across each film indicated the film resistance and thus its temperature. Each film was

calibrated over its full range of operating temperatures and a quadratic temperature-resistance relationship was established for each film. The measurement technique (see Measurement of T_0 and h) requires heat flux measurements at different surface temperatures. To generate the different surface temperatures, an external preheating unit was positioned over film 1, as illustrated in Fig. 1. This preheating unit was swung away just prior to the probes traversing the jet.

Measurement of T_0 and h

When the stagnation enthalpy of the flow is relatively high, it is usual to express the convective heat transfer in terms of an enthalpy difference across the stagnation point boundary layer [9]. However, because of the modest enthalpies encountered in the current application, the gases remain calorically perfect which means it is reasonable to express the stagnation point heat transfer as,

$$q = h(T_0 - T_w) \tag{1}$$

Due to the low velocity at the edge of the stagnation point boundary layer, it is appropriate for the stagnation temperature to appear in the governing relationship, Eq. (1). Since the entire length of each film cannot be precisely at the stagnation point, the flow velocity at the boundary layer edge will actually be nonzero for the majority of the film length. However, for the present films which were within 20deg of their respective stagnation points, the actual flow temperature at the edge of the boundary layer will be within about 0.5% of T_0, even for $M_\infty \to \infty$, the hypersonic limit [10]. (The hypersonic limit produces the largest departure of the recovery temperature from T_0 for a given distance from the stagnation point.)

A single transient thin film heat flux probe will produce measurements of both q and T_w, so if two thin films are operated at different values of T_w, then both h and T_0 can be identified since h is virtually independent of T_w in the current experiments (see Measurement of Concentration). In the current work, three films were operated at a number of different temperatures so that RMS measurements of fluctuations could be obtained.

Measurement of Concentration

This section demonstrates how the concentration of a binary gas mixture can be identified from the transient thin film heat transfer coefficient measurements. Theoretical results [9] suggest that the stagnation point heat transfer coefficient for a sphere at any Mach number can be correlated using,

$$Nu = 0.763 Pr^{0.4} Re^{0.5} C^{0.1} \left(\frac{KD}{u_\infty} \right)^{0.5} \tag{2}$$

where,

$$Nu = \frac{hD}{k_e} \tag{3}$$

$$Pr = \frac{c_p \mu_e}{k_e} \tag{4}$$

$$Re = \frac{\rho_e u_\infty D}{\mu_e} \tag{5}$$

$$K = \frac{\mathrm{d}u_e}{\mathrm{d}x} \tag{6}$$

$$C = \frac{\rho_w \mu_w}{\rho_e \mu_e}. \tag{7}$$

Pitot pressure measurements are routinely made in typical experiments, and the current work is no exception, so it is convenient to rearrange the heat transfer coefficient in terms of the Pitot pressure. Assuming measurements are made within a perfect gas, p_{pit} enters Eq. (2) through the Reynolds number (Eq. 5) using,

$$\rho_e = \frac{p_e}{RT_e} = \frac{p_{pit}}{RT_0}. \tag{8}$$

The undisturbed free stream Mach number is,

$$M_\infty = \frac{u_\infty}{(\gamma R T_\infty)^{0.5}} \tag{9}$$

and,

$$R = \frac{\gamma - 1}{\gamma} c_p. \tag{10}$$

Hence, it is possible to rearrange the heat transfer coefficient in Eq. (2) with the aid of Eqs. (8)–(10) as,

$$h = 0.763 D^{-0.5} f(M_\infty, \gamma) f(\text{thermophysical properties}) p_{pit}^{0.5} \tag{11}$$

where

$$f(M_\infty, \gamma) = \gamma^{0.5} (\gamma - 1)^{-0.25} (M_\infty)^{0.5} \left(\frac{T_\infty}{T_0} \right)^{0.25} \left(\frac{KD}{u_\infty} \right)^{0.5} \tag{12}$$

and

$$f(\text{thermophysical properties}) = c_p^{0.15} k_e^{0.6} \mu_e^{-0.1} C^{0.1} T_0^{-0.25} \tag{13}$$

Equation (12) indicates that for subsonic flows, the heat transfer coefficient is a strong function of the Mach number but it rapidly becomes independent of the Mach number for supersonic flows as illustrated in Fig. 2 for a flow with γ=1.4. Equation (12) is therefore an important result because it indicates that in supersonic flows, it is not necessary to have a precise measurement of the Mach number in order to estimate the stagnation point heat transfer coefficient with reasonable accuracy. To obtain the result presented in Fig. 2, the temperature ratio T_∞/T_0 in Eq. (12) was evaluated using the usual isentropic relationship, and the velocity gradient term was determined using,

$$\frac{KD}{u_\infty} \approx 3(1 - 0.252 M_\infty^2 - 0.0175 M_\infty^4) \quad \text{for } M_\infty < 0.8 \tag{15}$$

and

$$\frac{KD}{u_\infty} \approx \left(\frac{8 \rho_\infty}{\rho_e} \right)^{0.5} \quad \text{for } M_\infty > 1.2 \tag{16}$$

with an interpolation between Eq. (15) and Eq. (16) for $0.8 < M_\infty < 1.2$. The stagnation point velocity gradient expressions given by Eq. (15) and Eq. (16) are approximate relationships suggested by White [9].

If the Pitot pressure is measured and the Mach number has been identified such that $f(M_\infty, \gamma)$ is known with sufficient precision, then f(thermophysical properties) can be identified from the heat transfer coefficient measurements (Eq. 11) since the effective diameter of the probe is known or can be identified through a suitable calibration. The thermophysical properties of the flow are a function of the gas composition and Eq. (13) indicates that for gases with sufficiently dissimilar thermophysical properties, the measurement of convective heat transfer coefficient can be used to indicate the concentration of a binary gas mixture. Equation (13) is plotted in Fig. 3 as a function

of the mole fraction and mass fraction of a hydrogen-air mixture with T_0=290K and T_w=290K. In Fig. 3, the viscosity and conductivity of the hydrogen-air mixture have been evaluated using the Wilke formula.

Experiment and Data Acquisition

Experiments were performed using the free jet arrangement illustrated in Fig. 4. The contoured Mach 4 injection nozzle had a throat diameter of 9.42mm and was designed using the method of characteristics. The nozzle exit diameter was 29.5mm and the lip thickness was 0.5mm. The injection nozzle was located in the test section of the Oxford University Gun Tunnel. Either nitrogen or hydrogen was supplied to the Mach 4 nozzle from an unheated Ludwieg tube. Prior to a run, the test section was evacuated to approximately 1.2kPa, and the slug of gas in the Ludwieg tube was isolated from the low pressure test section by a fast-acting valve.

A short time after opening the fast-acting valve, a pressure rise was indicated by the injection pressure transducer and the injection static pressure measured 3mm upstream of the nozzle lip decreased during flow establishment and then increased back up to the steady injection value – see Fig. 5a. The Ludwieg tube filling pressure was chosen so that the steady injection static pressure was approximately the same as the initial test section pressure.

The thin film and Pitot pressure probes were initially located above the centreline of the jet and were driven across the jet at around 70ms after the fast-acting valve was opened – Fig. 5b. The traverse speed was approximately 1.7m/s and the physical separation of film 1 and the Pitot probe was 27mm. Traverses were performed at 4 locations: x=1, 100, 200, and 300mm. The Pitot pressure probe utilised a commercial piezoresistive transducer with a perforated screen and was about 2.5mm in diameter.

As previously mentioned, the measurement technique requires heat transfer measurements at different surface or film temperatures, and this was achieved in the current work using an external preheating unit as illustrated in Fig. 1. Although the preheating unit was positioned over film 1, the temperatures of films 2 and 3 also

increased through radiative heat transfer from the unit. The temperature of film 1 was monitored during the preheating process, and when the required surface temperature was achieved, a run was manually initiated.

Prior to sampling, the amplified signal from the Pitot probe was low pass filtered with a cut-off frequency of about 60kHz. Signals from all transducers were recorded at 8kSamples/s and subsequently analysed to yield the time averaged results. For the analysis of fluctuating results, signals from the thin film temperature probes were processed by electrical heat transfer analogue units [11], and were then sampled at 500kSamples/s. The bandwidth of the heat transfer analogue units extends to about 85kHz.

The matching of injection static pressure and test section pressure remains somewhat uncertain because during a traverse of the jet, the test section pressure transducer registered a value lower than the initial test section pressure prior to flow establishment (Fig. 5a). During the traverse, the average test section pressure registered by the transducer was 1.05kPa for the nitrogen jet and 1.08kPa for the hydrogen jet. The difference between injection and test section pressures leads to the development of shock-expansion cells within the jet flow and some uncertainty in the static pressure within the jet for x=100, 200, and 300mm stations. The shock and expansion waves appear to have little influence on any of the probe measurements; no such waves were visible in schlieren flow visualisation of the jet flows.

Estimates of the Mach 4 nozzle exit flow parameters are presented in Table 1. These values are based on measurements of the static pressure, Pitot pressure, and the flow total temperature as discussed in the next section. The uncertainties quoted in Table 1 are based on the estimated uncertainties and spatial variation of the measured quantities at x=1mm. For the stations: x=100, 200, and 300mm, the uncertainty in static pressure is ±14% for the nitrogen jet and ±32% for the hydrogen jet (substantially larger than quoted in Table 1) due to the mismatch of pressures discussed previously. These uncertainties in static pressure are substantial, but it is still possible to extract meaningful results from the measurements, as will be demonstrated in the remainder of this article.

Time-averaged Results

Transient Heat Flux Analysis.

The transient thin film heat flux probes provide a measurement of probe surface temperature that must be converted into a heat flux using an appropriate model for the transient heat conduction processes within the probe substrate. In the present work, the heat flux was identified from the surface temperature signals using a finite difference routine [12] which accounts for the temperature-dependent thermal properties and the hemispherical geometry of the quartz substrates. It is important to properly account for the temperature-dependent thermal properties of the quartz because of the elevated surface temperatures encountered during the experiments and large probe surface temperature variations during jet traverses, particularly in the case of the hydrogen jet, Fig. 5c. The hemispherical geometry can also be significant because the heat penetrates a significant distance relative to the probe radius during the 50ms or so taken by the probe to traverse the jet, Fig. 5.

Typical examples of thin film temperature and corresponding heat flux measurements are illustrated in parts c and d of Fig. 5. The minimum heat flux (Fig. 5d) occurs earlier than the minimum probe surface temperature (Fig. 5c) because in its simplest form, the heat flux can be expressed as an integral involving the derivative of the surface temperature [12].

The time-averaged components of the probe temperature and heat flux data were identified by digitally low-pass filtering the data such as that illustrated in Fig. 5c and d. The cut-off frequency of the digital filter was varied with the traverse location: 1.0kHz for x=1mm, 0.5kHz for x=100mm, 0.2kHz for x=200mm, and 0.1kHz for x=300mm.

Stagnation Temperature and Heat Transfer Coefficients.

At each of the 4 locations downstream of injection (x=1, 100, 200, and 300mm), a number of traverses – either 3 or 4 – were performed at different initial probe temperatures. In principal, only two different probe temperatures are required for the identification of the flow total temperature and heat transfer coefficient (see

Measurement of T_0 and h). However, as the spatial separation of the thin film probes was on the order of 10mm, which is on the same order as the half-width of the jet, the fluctuations in heat flux at the different probes are poorly correlated so it is necessary to adopt an RMS analysis for the identification of fluctuations. While, the motivation for the use of multiple probe temperatures was principally the RMS fluctuation analysis, the analysis of the time-averaged results is also enhanced by the additional data at different probe temperatures. The same results could have been obtained using a single probe traversing the jet a number of times. The use of multiple probes within the same device reduced the number of traverses that were required.

To identify the flow stagnation temperature and probe heat transfer coefficient distribution at each traverse location, the spatial variation of the probe temperature and heat flux data from each probe was referenced to the centre line of the jet via the appropriate probe displacement measurement (eg, Fig. 5b). A linear regression for the heat flux versus probe temperature data was performed at each position across the jet. Figure 6 illustrates the regression at two locations across the hydrogen jet at x=300mm. The data presented in this figure were obtained from three traverses of the jet at the points in time when each film passed the locations y=0 and y=-20mm. The film temperatures appear to be almost identical at these locations (y=0 and y=-20mm) because the transient response of the films to the convective cooling resulted in relatively small differences in film temperature at the indicated locations (see Fig. 5 parts b and c). The intercept of the regression line and the vertical axis indicates the flow stagnation temperature (at that point within the jet) and the inverse of the slope of each regression line indicates the heat transfer coefficient of the probes (at that point within the jet).

The stagnation temperature and heat transfer coefficient results obtained in this manner are presented in Fig. 7 and Fig. 8. The bars illustrated on these figures indicate the magnitude of the 95% confidence intervals derived from the statistical analysis of the linear regression data (eg, see Chatfield [13]). At the center of the nitrogen and hydrogen jets, the estimated uncertainty derived from this regression analysis was around ±5K for the stagnation temperature, and ±3.5% for the heat transfer coefficient. Generally, the relative measurement uncertainty in both

stagnation temperature and probe heat transfer coefficient increases with distance from the jet center line because the magnitude of the heat flux approaches zero (Fig. 5). For example, see the bars reported in Fig. 7 and Fig. 8 at x=300mm. The average uncertainties at y=±20mm are ±10K and ±6% in stagnation temperature and heat transfer coefficient respectively.

The stagnation temperature measurements for the hydrogen jet, Fig. 7, indicate the existence of significant spatial variations on the order of ±10K. Similar results are obtained in the nitrogen jet, but the variations are less significant [14]. Spatial variations in the stagnation temperature of jet flows have previously been observed in subsonic [15] and Mach 2 [16] jet flows. Such effects have been described as "temperature separation" and can be explained in terms of either vortex or shock-vortex interaction processes [15,16].

Concentration Measurements.

Concentration can be identified from the heat transfer coefficient measurements provided the Pitot pressure is measured and Mach number is known to a reasonable precision, as indicated by Eq. (11). The distribution of flow properties identified from the Pitot probe (as with the data from the 3 heat transfer probes) are referenced to the jet center line with the aid of the probe displacement measurement for each traverse (eg, Fig. 5b).

Pitot pressure measurements within the nitrogen jet were combined with static pressure measurements in order to identify the Mach number distribution within the jet flow. Static pressure was taken as equal to the value indicated by the injection static pressure transducer for the traverse at x=1mm, however, for the remaining traverse stations (x=100, 200, and 300mm), the static pressure within the jet was taken as the average value between the injection static pressure and the test section pressure values. The function described in Eq. (13) was then evaluated for the nitrogen using Sutherland's law for the viscosity and conductivity, assuming the flow stagnation and probe temperatures were both 290K.

The heat transfer coefficient (Eq. 11) was then evaluated with the effective probe diameter D taken as 2.88mm. The diameter of 2.88mm was chosen so that the convective heat transfer coefficient predictions in the nitrogen jet at x=1mm matched the thin film measurements, Fig. 8a. The 3mm diameter is only nominal and the stagnation point radius of curvature is generally less than 1.5mm for these devices [17]. Thus, the nitrogen jet at x=1mm has been used to calibrate the probes – an effective diameter of 2.88mm is physically reasonable.

At subsequent stations in the nitrogen jet (Fig. 8c, e, and g) predicted heat transfer coefficient distributions are in close agreement with the distributions identified from the thin film probes. Differences between the predictions and the measurements are apparent in the outer regions of the jet, for example, for y > 20mm in Fig. 8e and Fig. 8g. In these regions the Mach number is transonic or subsonic, and hence inaccuracies in the Mach number estimate (which arise due to uncertainties in the flow static pressure) will have a strong influence on the heat transfer coefficient prediction (Eq. 12, Fig. 2). Another obvious deviation between the measured and predicted results occurs at x=200mm (Fig. 8e) towards the center of the jet. The magnitude of this deviation is on the same order as the estimated uncertainty in the thin film heat transfer coefficient measurements of around 3.5% near the center of the jet.

In the case of the hydrogen jet, Mach number distributions were identified from the pressure measurements as for the nitrogen jet. In Fig. 8, two heat transfer coefficient predictions based on the Pitot pressure measurements and Eq. (11) are presented. The higher of the two heat transfer coefficient predictions is for the case of pure hydrogen, and lower result is for the case of air. Clearly, the thin film heat transfer coefficient measurements in the hydrogen jet generally fall between these two limits.

To identify the concentration of hydrogen at each position, the value of f(thermophysical properties) was effectively evaluated using Eq. (11) with the thin film value of h, the measured values of p_{pit}, the Mach number distribution estimated using the ratio of Pitot and static pressure, and D=2.88mm (identified from the nitrogen jet experiments). Having obtained f(thermophysical properties), the concentration of hydrogen was identified from Eq. (13) which is principally a

function of concentration as illustrated in Fig. 3. Results from the concentration analysis are presented in Fig. 9 at each station downstream of injection in terms of both mole fractions (the solid lines) and mass fractions (the dots).

On the jet center line, the results in Fig. 9 indicate that the hydrogen concentration is around 0.998 in terms of mole fractions, or around 0.98 in terms of mass fraction. It is expected that the actual hydrogen concentration in the jet core was X_{H2}>0.999 or Y_{H2}>0.99 because high purity hydrogen was used and care was taken to evacuate and thoroughly flush out the Ludwieg tube prior to final filling with the hydrogen. The fact that the concentration of hydrogen within the core was $Y_{H2}\approx 0.98$ is indicative of the level of accuracy that can be anticipated with this technique, rather than a contaminated hydrogen stream.

The primary source of uncertainty in the measurement of concentration is the measurement of the thin film convective heat transfer coefficient of the probes and the estimation of $f(M_\infty, \gamma) \times p_{pit}^{0.5}$ using the Pitot and static data. The uncertainty in the thin film heat transfer coefficient measurements has been estimated as around ±4% in the jet core and uncertainty in $f(M_\infty, \gamma) \times p_{pit}^{0.5}$ predictions based on p_{pit} and p_∞ is estimated as around ±3%. This leads to an uncertainty in the value of *f*(thermophysical properties) of around ±5% within the jet core. Given *f*(thermophysical properties) remains a reasonably linear function of hydrogen mass fraction, Fig. 3, the uncertainty in Y_{H2} remains at around ±5% over the entire range of concentrations. However, as *f*(thermophysical properties) is a far more nonlinear function of hydrogen concentration when expressed on a mole basis (Fig. 3), the uncertainty in mole fraction varies between about ±2% for X_{H2}=0.9 up to about ±25% for X_{H2}=0.4, assuming the uncertainty in *f*(thermophysical properties) remains at ±5% over this range of concentrations.

Fluctuation Results

Transient Heat Flux Analysis.

High bandwidth stagnation point heat flux results were identified from the analogue voltage signals using an appropriate analogue sensitivity which varied with the time-averaged probe temperature. This is a reasonable approach because at frequencies

higher than about 1kHz, the heat penetrates only a small distance relative to the probe radius, and the associated temperature fluctuations are not large enough to induce significant variable thermal property effects. Similar approaches have been used in previous studies with transient thin film probes [14,17].

Fluctuations in the stagnation point heat flux were then identified by treating the sampled high bandwidth signals with the digital filters discussed previously (see Time-Averaged Results) in order to first identify a time-averaged result. This time-averaged result was then subtracted from the original high bandwidth results to obtain the fluctuating component.

Fluctuation Analysis.

Resolving the total stagnation point heat flux into mean and fluctuating components,

$$q = \bar{q} + q' \tag{17}$$

and treating the heat transfer coefficient and temperatures in Eq. (1) in a similar manner, it is found that the fluctuations in the heat flux are related to the fluctuations in heat transfer coefficient and stagnation temperature according to,

$$\frac{\overline{q'^2}}{\bar{h}^2} \approx \frac{\overline{h'^2}}{\bar{h}^2}\left(\overline{T_0} - \overline{T_w}\right)^2 + 2\frac{\overline{h'T_0'}}{\bar{h}}\left(\overline{T_0} - \overline{T_w}\right) + \overline{T_0'^2} \tag{18}$$

To achieve the result expressed in Eq. (18), it was necessary to neglect higher order terms and to recognise that the probe temperature fluctuations T_w' are less than 0.4% of $q'/\bar{h}$ for the present conditions, and hence can be neglected.

If the heat flux probes are operated at a temperature very close to the flow stagnation temperature, then Eq. (18) indicates that the RMS stagnation temperature fluctuations can be directly identified from the fluctuations in heat flux and the time-averaged heat transfer coefficient measurements according to,

$$\left(\overline{T_0'^2}\right)^{1/2} \approx \left(\frac{\overline{q'^2}}{\bar{h}^2}\right)^{1/2} \tag{19}$$

If a number of different thin film probe operating temperatures are used, then each of the fluctuation terms on the right hand side of Eq. (18) can be identified from the measured fluctuations in the stagnation point heat flux and the measured time-

averaged quantities. In supersonic flows, the fluctuations in the heat transfer coefficient will be primarily due to fluctuations in concentration and Pitot pressure, since the sensitivity to fluctuations in Mach number is low for supersonic flows, Eq. (12) or Fig. 2. However, the actual magnitude of the concentration fluctuations cannot be easily identified using the current approach because the term, $\overline{f'(\text{thermophysical properties})p_{pit}'}$ cannot be readily estimated.

If fluctuations in concentration are of interest in future applications, a better approach would be to reduce the spatial separation of the thin film probes and Pitot probe. A spatial separation of heated and unheated films of around 1mm has already been demonstrated [10]. Inclusion of a Pitot probe in close proximity to such a configuration would allow instantaneous concentration measurements to be made and by-pass the treatment of fluctuations using mean-square quantities. However, for the time being, fluctuation measurements from the probe are restricted to stagnation temperature fluctuation results.

Results

Stagnation temperature fluctuations identified from the probe measurements according to Eq. (19) are presented in Fig. 10 for three different probe temperatures ranging from $\overline{T_w}$ =315 to 350K. Taking the time-averaged flow stagnation temperature as around $\overline{T_0}$ =290K (a reasonable approximation for *x*=100, 200, and 300mm, Fig. 7), the difference $(\overline{T_0} - \overline{T_w})$ for the data represented by the different lines in Fig. 10 typically varies between about -25 and -60K. Given that the stagnation temperature results identified using Eq. (19) are very similar regardless of the actual probe temperatures within this range, it is concluded that results in Fig. 10 are a good representation of the actual stagnation temperature fluctuations.

The largest difference in RMS stagnation temperature fluctuations identified by using the different probe temperatures occurs at *x*=300mm, Fig. 10. At this station, stagnation temperature fluctuations were also identified by curve fitting a quadratic function to the $(\overline{T_0} - \overline{T_w})$ versus $\overline{q'^2}/\overline{h}^2$ data for all of the probe temperatures up to $\overline{T_w} \approx 610$K as suggested by Eq. (18). Results from this quadratic analysis are

presented in Fig. 11 where a comparison is made with results obtained using the approximation given in Eq. (19). These results provide additional confirmation that the results in Fig. 10 are a valid representation of the actual stagnation temperature fluctuations.

Conclusions

The present work introduces a new concentration probe measurement technique for use in binary gas flows. The technique is based on the measurement of the convective heat transfer coefficient associated with nominally identical stagnation point transient thin film heat flux gauges. Pitot pressure measurements are used in conjunction with a heat transfer correlation and the heat transfer coefficient measurements to identify the concentration of the mixture. The stagnation point heat transfer correlation indicates that at supersonic speeds the convective heat transfer coefficient is virtually independent of the flow Mach number. Thus, it is not essential to have accurate measurements of static pressure provided the binary gas flow is supersonic.

As a demonstration of the new technique, the probe was operated in Mach 4 nitrogen and hydrogen free jets issuing into a low pressure air environment. The nitrogen jet results demonstrated that accurate predictions of the thin film probe heat transfer coefficient were made within the supersonic portion of the jet based on Pitot pressure measurements and estimates of the static pressure within the jet. When the probe was applied in the hydrogen jet, concentration measurements of around Y_{H2}=0.98 were obtained within the jet core flow – a slightly lower hydrogen concentration than anticipated. However, this result is quite good considering that the uncertainty in mass fraction measurement is estimated as around ±5% for the technique in its present application. Hydrogen concentration measurements are presented for four stations downstream of the Mach 4 nozzle: x=1, 100, 200, and 300mm.

Stagnation temperature measurements have also been obtained using the probe. Although there was reasonable spatial uniformity of stagnation temperature across the hydrogen jet core flow at x=1mm, significant peaks and troughs are apparent at the downstream stations. Similar spatial distributions of stagnation temperature have

been observed previously in free jets flows at much lower Mach numbers and have been attributed to vortex-induced energy separation effects [15,16]. RMS fluctuations in stagnation temperature have also been identified from the probe measurements. At the exit of the injection nozzle, RMS fluctuations of around 1K are apparent, while at the last station (x=300mm), RMS fluctuations of between about 5K and 15K occur within the central portion (y<±20mm) of the hydrogen jet flow.

The thin film probes are robust and have a frequency response that extends to around 100kHz, and the measurement technique appears well suited to supersonic flow environments. However, two factors that may preclude the application of the present concentration probe arrangement in other supersonic mixing configurations are: 1) the absence of a local static pressure measurement; and 2) the operation of the external preheating unit. An additional cone or wedge pressure probe could be incorporated into the arrangement in cases where local static pressure measurements are necessary. The external preheating unit could be replaced by an internal heating system in a hollow quartz probe [17], or by exciting one film with a relatively high current pulse [10]. The pulsed heating arrangement of [10] offers the additional advantage of higher spatial resolution, and if a pitot pressure transducer were incorporated into such a configuration, instantaneous measurements of concentration would also be possible.

Nomenclature

c_p specific heat
C Chapman-Rubesin parameter, defined in Eq. (7)
D probe diameter
h convective heat transfer coefficient
k conductivity
K stagnation point velocity gradient, defined in Eq. (6)
M Mach number
n exponent in power law viscosity expression
Nu Nusselt number, defined in Eq. (3)
p pressure

Pr Prandtl number, defined in Eq. (4)

q surface heat flux

R specific gas constant

Re Reynolds number, defined in Eq. (5)

T temperature

T_0 stagnation temperature

u velocity

x distance from jet exit, or distance along probe surface from stagnation

X mole fraction

y distance from jet centreline

Y mass fraction

γ ratio of specific heats

μ viscosity

ρ density

Subscripts

e boundary layer edge

pit Pitot

w surface value

∞ undisturbed free stream

References

[1] McQuaid, J., and Wright, W., 1973, "The Response of a Hot-Wire Anemometer in Flows of Gas Mixtures," Int. J. Heat Mass Trans. **16**, pp 819-828.

[2] McQuaid, J., and Wright, W., 1974, "Turbulence Measurements with Hot-Wire Anemometry in Non-Homogeneous Jets," Int. J. Heat Mass Trans. **17**, pp 341-349.

[3] Brown, G. L., and Rebollo, M. R., 1972, "A Small, Fast-Response Probe to Measure Composition of a Binary Gas Mixture," AIAA J. **10**, 649-652.

[4] Swithenbank, J., 1977, "Measurement in Combustion Processes," in "Measurement of Unsteady Fluid Dynamic Phenomena," B. E. Richards (Ed.), Hemisphere, pp. 189-212.

[5] Ninnemann, T. A., and Ng, W. F., 1992, "A Concentration Probe for the Study of Mixing in Supersonic Shear Flows," Experiments in Fluids **13**, pp 98-104.

[6] Ng, W. F., and Epstein, A. H., 1983, "High-Frequency Temperature and Pressure Probe for Unsteady Compressible Flows," Rev. Sci. Instrum. **54**, pp 1678-1683.

[7] VanZante, D. E., Suder, K. L., Strazisar, A. J., and Okiishi, T. H., 1994, "An Improved Aspirating Probe for Total-Temperature and Total-Pressure Measurements in Compressor Flows," ASME Paper 94-GT-222.

[8] Buttsworth, D. R., and Jones, T. V., 1998, "A Fast-Response Total Temperature Probe for Unsteady Compressible Flows," J. Engineering for Gas Turbines and Power **120**, pp 694-702.

[9] White, F. M., 1991, "Viscous fluid flow," 2nd ed., McGraw Hill.

[10] Buttsworth, D. R., and Jones, T. V., 1998, "A Fast-Response High Spatial Resolution Total Temperature Probe using a Pulsed Heating Technique," J. Turbomachinery **120**, pp 601-607.

[11] Oldfield, M. L. G, Burd, H. J., and Doe, N. G., 1982, "Design of Wide-Bandwidth Analogue Circuits for Heat Transfer Instrumentation in Transient Wind Tunnels," Proceedings 16th Symp. of International Centre for Heat and Mass Transfer, Hemisphere Publishing, pp. 233-257

[12] Buttsworth, D. R., 2001, "A Finite Difference Routine for the Solution of Transient One Dimensional Heat Conduction Problems with Curvature and Varying Thermal Properties," Technical Report TR-2001-01, Faculty of Engineering and Surveying, University of Southern Queensland.

[13] Chatfield, C., 1970, "Statistics for Technology," Penguin.

[14] Buttsworth, D. R., and Jones, T. V., 2001, "Transient Temperature Probe Measurements in a Mach 4 Nitrogen Jet," submitted to Experiments in Fluids.

[15] Fox, M. D., Kurosaka, M., Hedges, L., and Hirano, K., 1993, "The Influence of Vortical Structures on the Thermal Fields of Jets," J. Fluid Mech. **255**, pp 447-472 (and corrigendum **261,** p 376).

[16] Fox, M. D., and Kurosaka, M., 1996, "Supersonic Cooling by Shock-Vortex Interaction," J. Fluid Mech. **308**, pp 363-379.

[17] Buttsworth, D. R., Jones, T. V. and Chana, K. S., 1998, "Unsteady Total Temperature Measurements Downstream of a High Pressure Turbine," J. Turbomachinery **120**, pp 760-767.

Table 1 Injection parameters

Parameter	Nitrogen Jet	Hydrogen Jet
M_∞	3.7 ± 0.1	3.8 ± 0.1
T_∞ (K)	78 ± 4	72 ± 4
p_∞ (kPa)	1.20 ± 0.04	0.81 ± 0.07
u_∞ (m/s)	664 ± 10	2450 ± 40
ρ_∞ ($\times 10^{-3}$ kg/m^3)	52 ± 3	2.7 ± 0.3

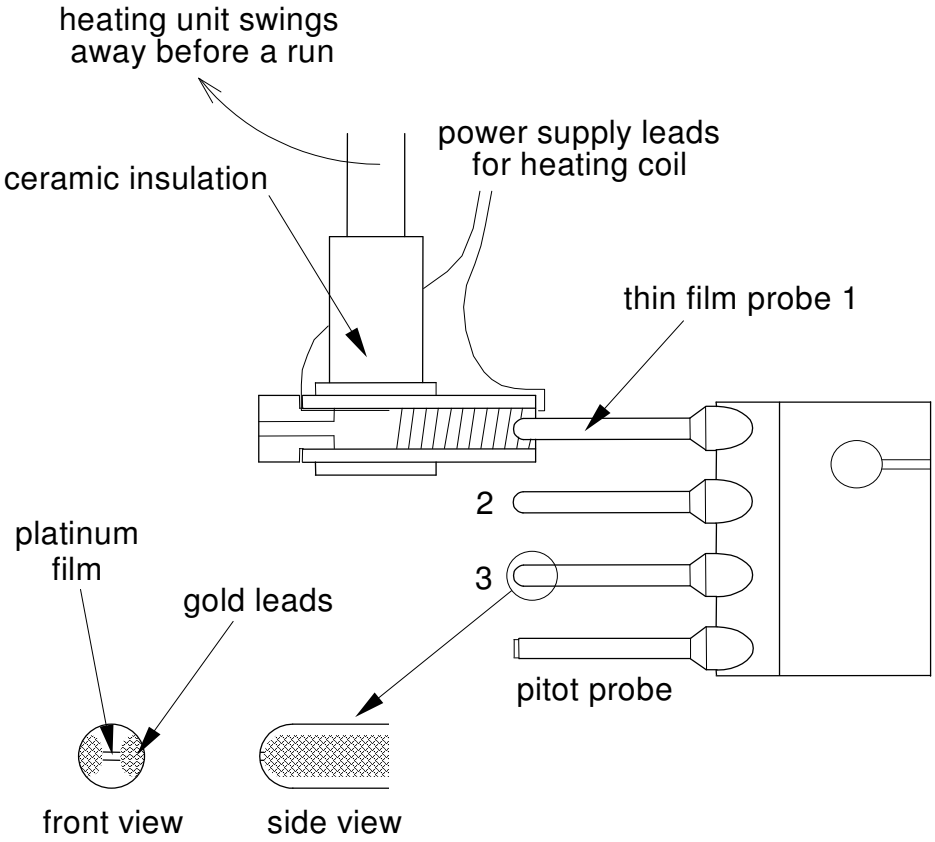

Fig.1 Illustration of the probe arrangement

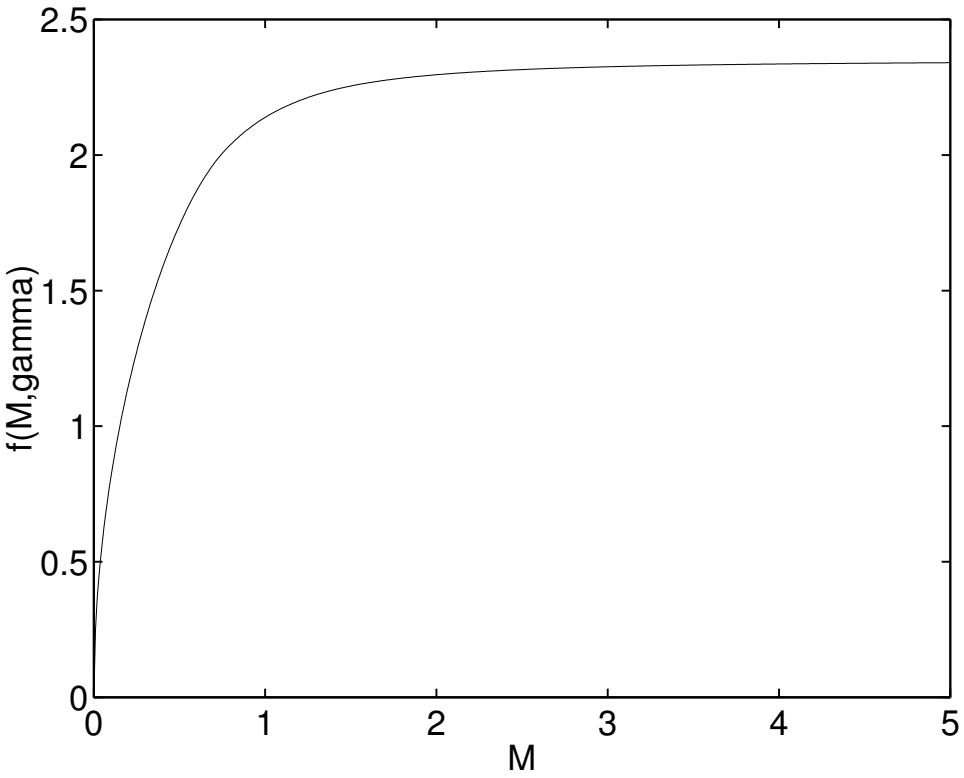

Fig. 2 Sensitivity of heat transfer coefficient to Mach number as indicated by $f(M_\infty,\gamma)$ for γ=1.4

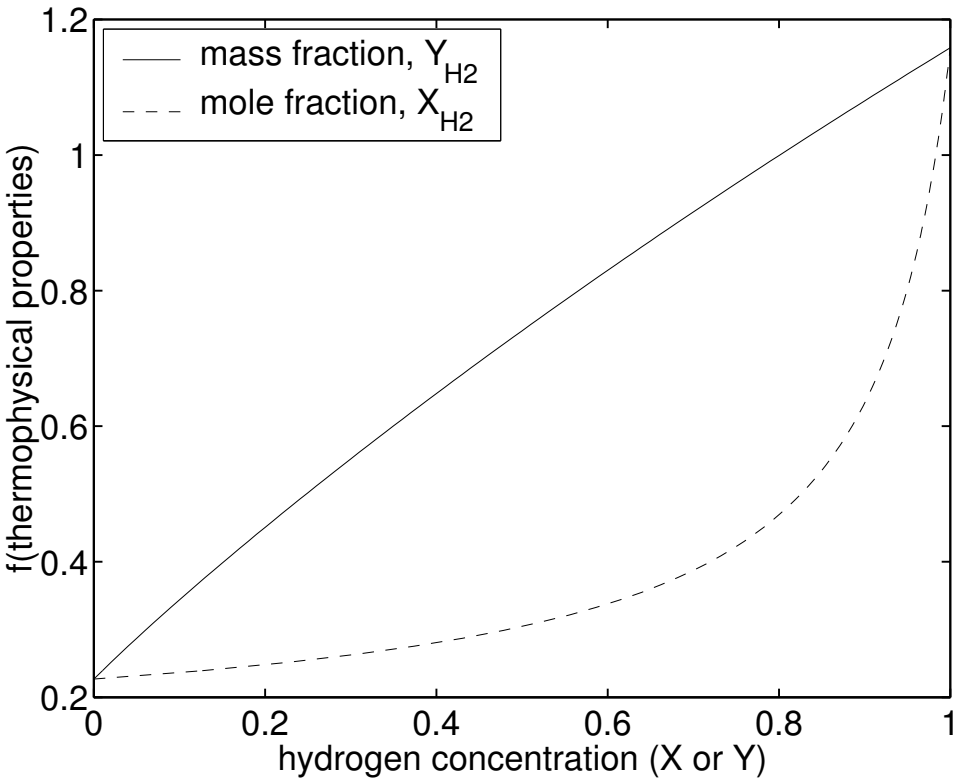

Fig. 3 Sensitivity of heat transfer coefficient to the concentration of the mixture as indicated by *f*(thermophysical properties) for a hydrogen-air mixture at T_0=290K.

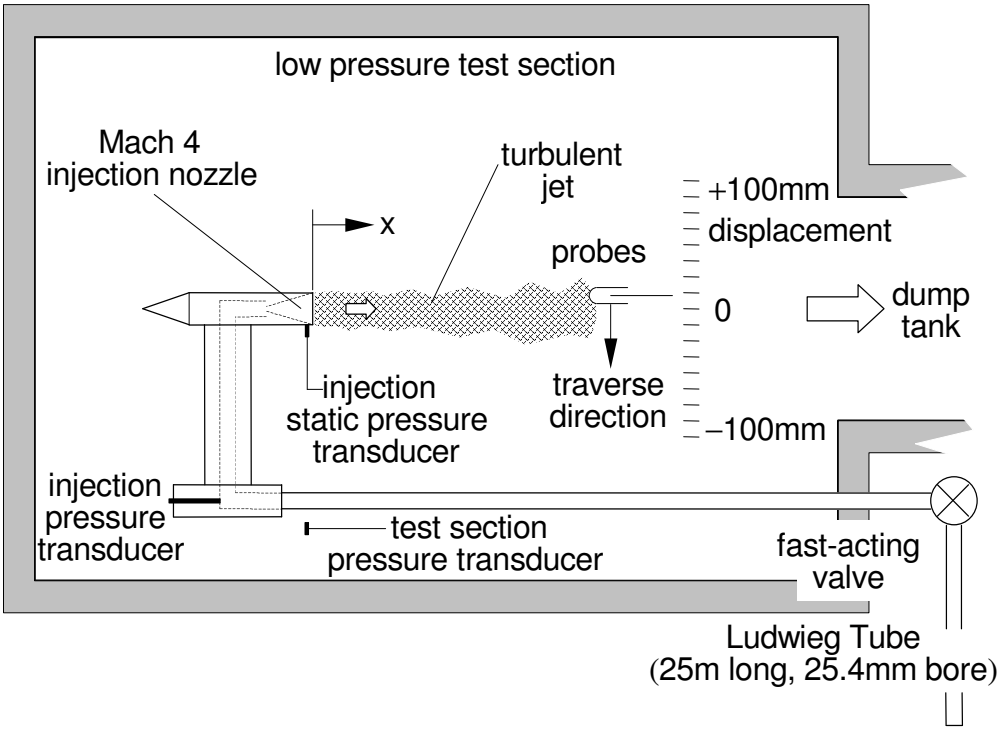

Fig. 4 Illustration of the Mach 4 free jet arrangement

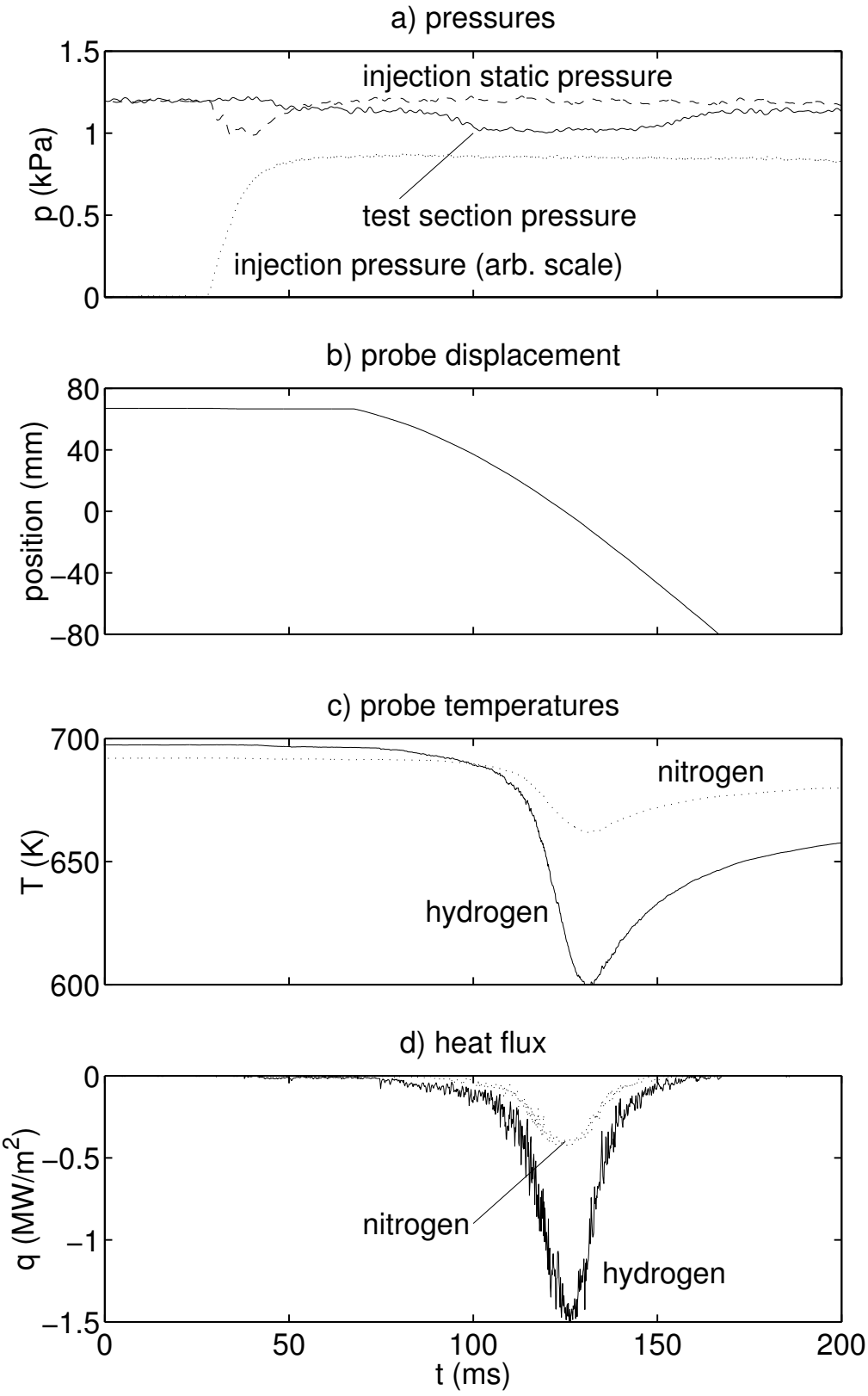

Fig. 5 Typical signals obtained during the experiments

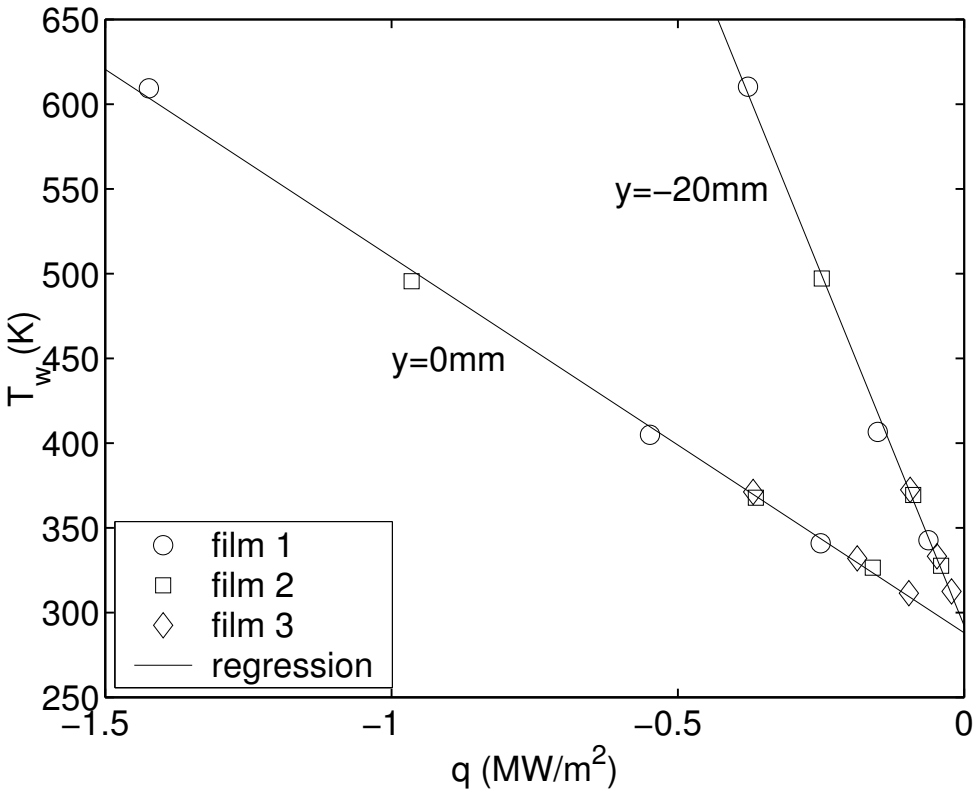

Fig. 6 Illustration of heat flux for various probe temperatures at two points across the hydrogen jet for x=300mm

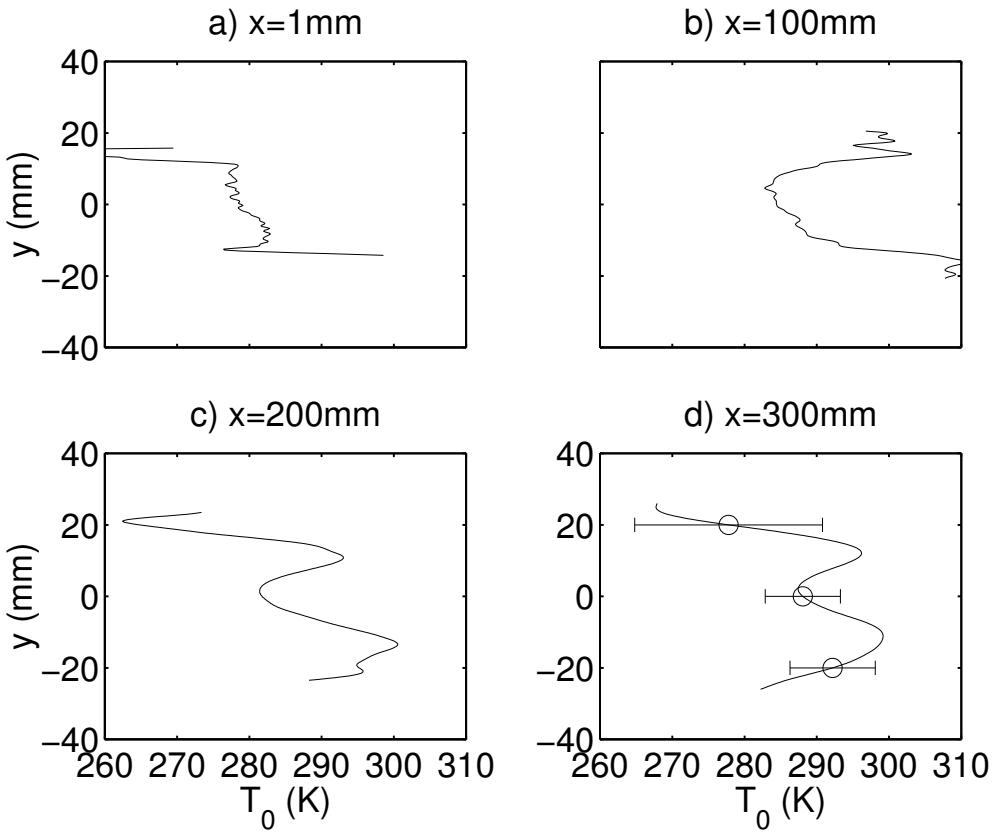

Fig. 7 Time-averaged stagnation temperature measurements in the hydrogen jet at 4 stations downstream of injection

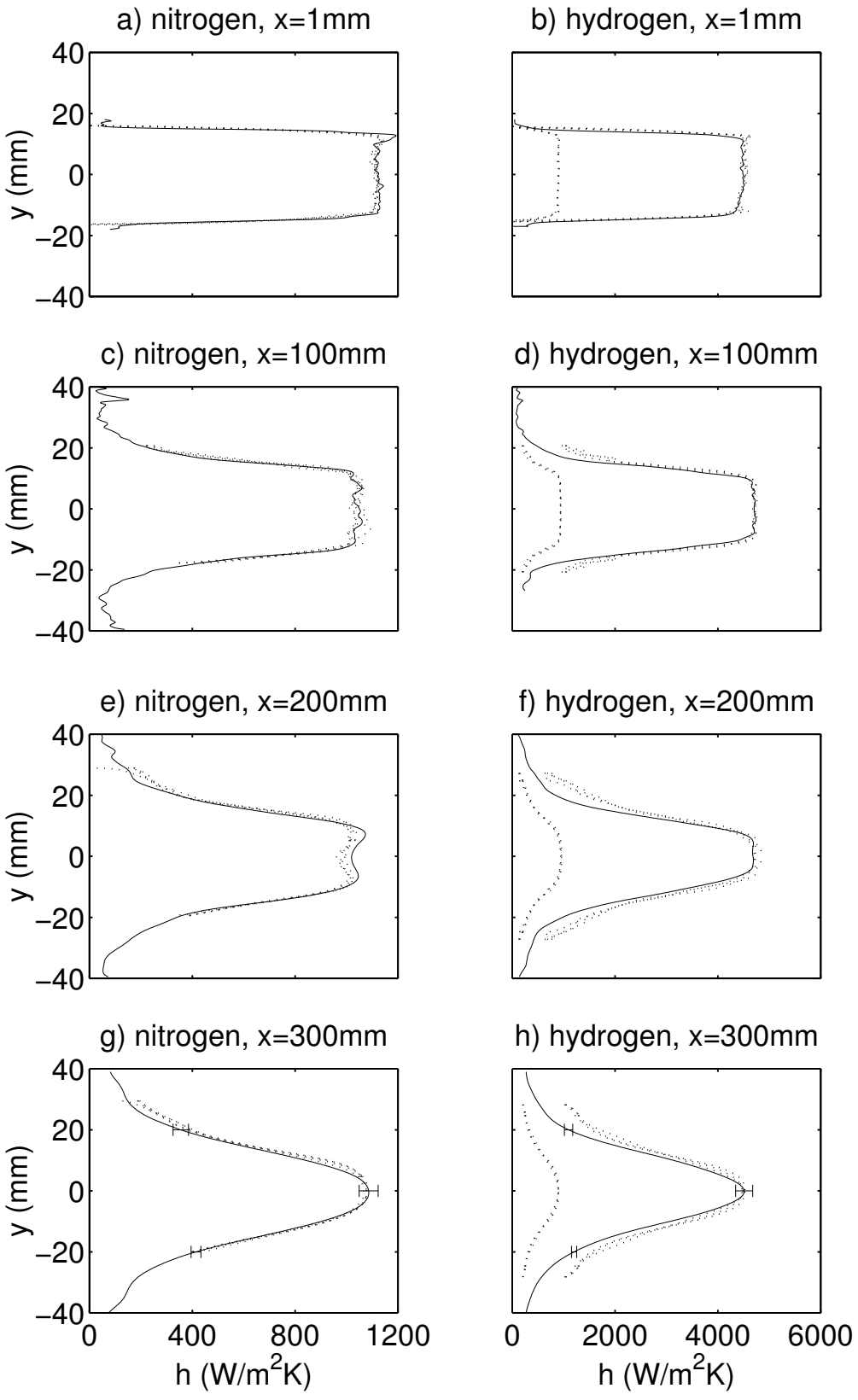

Fig. 8 Time-averaged heat transfer coefficient results at 4 stations downstream of injection. Solid lines: thin film probes; dots: Pitot probe predictions

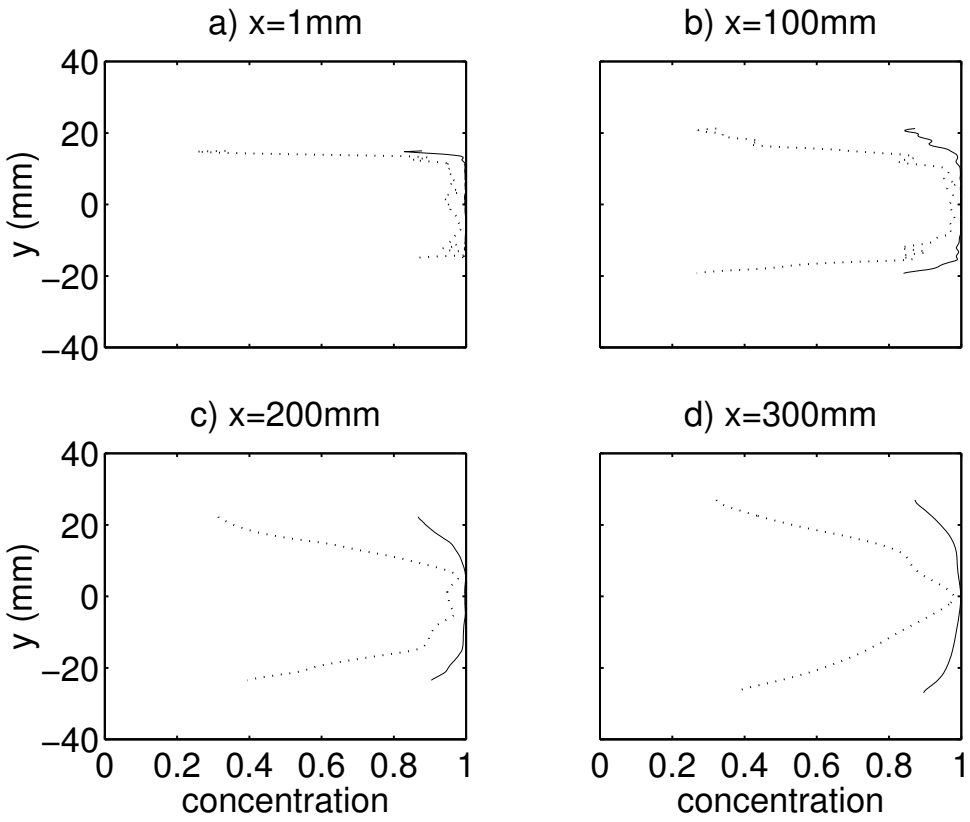

Fig. 9 Time-averaged hydrogen concentration profiles. Solid line: hydrogen mole fraction; dots: hydrogen mass fraction

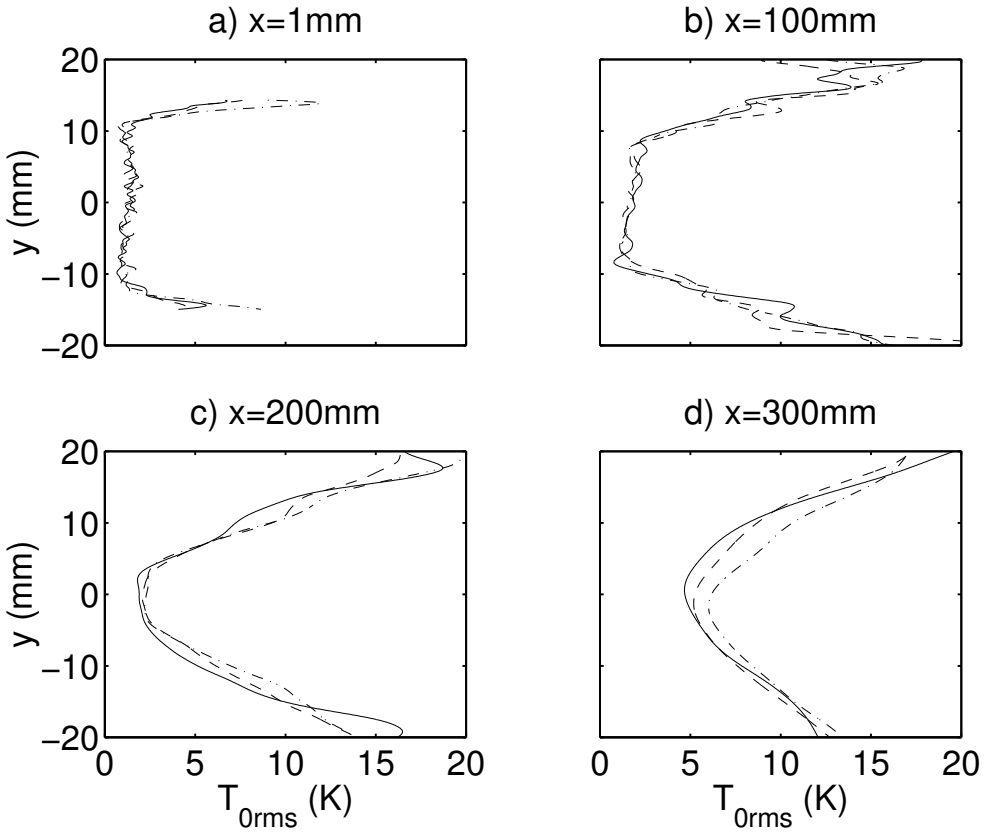

Fig. 10 Stagnation temperature fluctuations at 4 stations downstream of injection for three different values of T_0-T_w

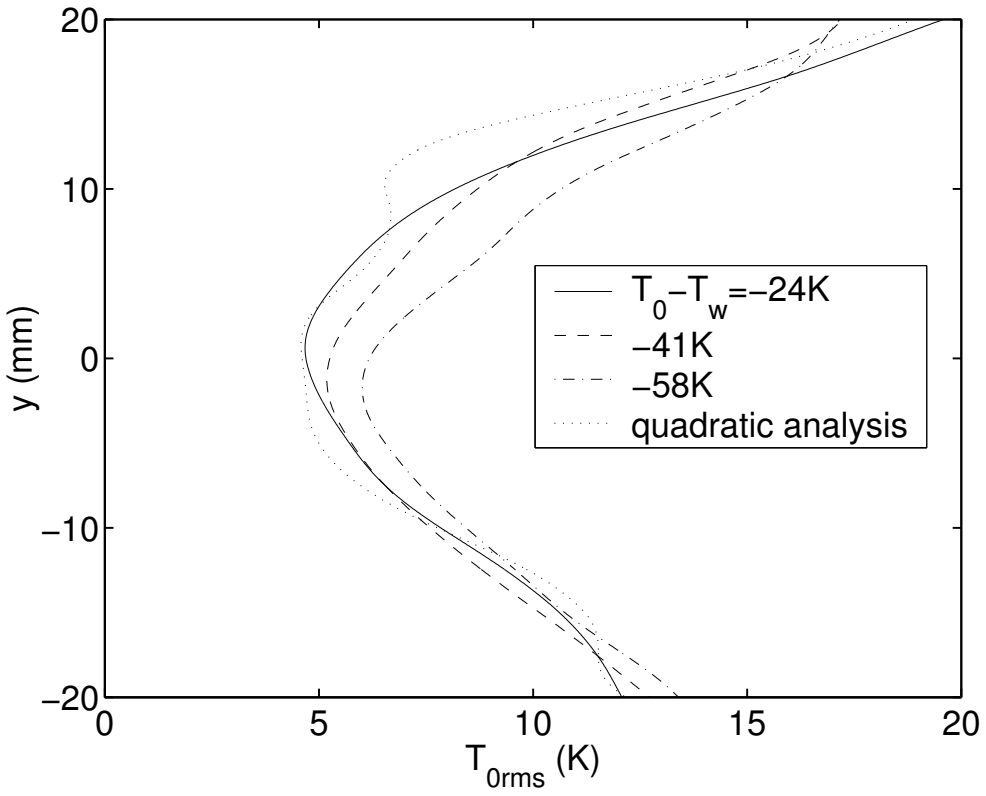

Fig. 11 Stagnation temperature fluctuations in the hydrogen jet at x=300mm.